# Experimental Investigation Thermal Performance of Loop Heat Pipe Operating with Different Working Fluids

Phuoc Hien Huynh[1], Kyaw Zin Htoo[1], Keishi Kariya[2] and Akio Miyara[2,3,*]

[1]*Saga University, Graduate school of Science and Engineering, Saga, Japan*

[2]*Saga University, Department of Mechanical Engineering, Saga, Japan*

[3]*International Institute for Carbon – Neutral Energy Research, Kyushu University, Fukuoka-shi, Japan*

**Abstract:** Nowadays, due to the tremendous development of data centers (DCs), studying the effective cooling methods that can face to the challenges such as the high power or heat flux dissipation and the efficient electricity consumption in DCs has never been unnecessary. Loop heat pipe (LHP), a two-phase heat transfer device, is being considered as one of the potential solutions for the above problems. This paper introduces the experimental study on the thermal performances of LHP functioning under gravity assisted condition with different working fluids that are water and ethanol ($C_2H_5OH$). This LHP has the flat-rectangular evaporator with the stainless-steel (SS) sintering wick installed inside. The results demonstrate that under the same condenser cooling condition, water LHP performed better than ethanol LHP. In the case of water LHP, when heating power was increased from 33 to 535 W, the temperature at the top surface of the heating block raised from 38°C to 110°C. With the ethanol LHP, this temperature reached 133°C at the heating power of 395 W. If temperature limitation of microprocessors functioning inside the DCs is recognized at 85°C, the cooling capabilities of LHP are 220 W and 350 W corresponding to the working fluid are ethanol and water respectively. In addition, the discussions about the difference in boiling heating transfer characteristics as well as condenser performances between water LHP and ethanol LHP are also presented in this study.

**Keywords:** Electronics cooling, Loop heat pipe, Working fluids, Gravity assisted condition, Water, Ethanol, Boiling heat transfer, Condensation heat transfer.

## 1. INTRODUCTION

In recent decades, the techniques including online searching engine, social networking, cloud computing, and etc. have approached the great progress and become inseparable from human daily activities. Although this tendency promotes the development of data centers (DCs) industry, it also causes some serious challenges to this field, especially some belonging to the cooling or thermal management system. Because the DC is a facility housing various kind of computers and servers at the high density for collecting, storing, managing, disseminating data, and operating with the downtime to be near to zero, it requires that the cooling system has the reliable and stable performance. Moreover, within the miniaturizing characteristic of the electronics such as microprocessors, the thermal power and heat flux generated from the devices increases dramatically with time. In the 1960s, there were only 50-1000 components on one chip; however, since 2006 a chip with 100 million transistors per square of centimetre had been manufactured. It is predicted that the power generated from the chip can reach 350 W by 2020 [1]. Besides, the explosion in demand on using the Internet also causes the number of DCs and their electricity consumption expand quickly. In accompany with it, electricity consumption and environmental impact become the concerns in the field of DCs. Recent energy statistics show that from 2000 to 2005, DCs electricity consumption increased twice, and continued growing up at the rate of 10% per year five years later. In 2010, DCs was responsible for 1.1% to 1.5% of the global and 2% of US electricity consumption. As a result, the emission of $CO_2$ from DCs activities has been increasing. In 2002 the global DCs footprint was 76 $MtCO_2e$ and it is expected to reach the value of 259 $MtCO_2$ in 2020 or grow up at the rate of 7% per year [2]. It is also indicated that normally, around 40% of electricity consumption by DCs is used by the mechanical equipment such as chiller, blower or cooling tower [2-4], so it is possible to cut down the electricity consumption significantly by improving the cooling system. Therefore, the modern cooling method has not only the reliable, sufficient cooling capacity but also being friendlier with the environment or saving electricity consumption characteristics.

From the mentioned problems, LHP, a novel catalogue of the heat pipe (HP), can be considered as one of the potential solutions. LHP is also a passive two-phase heat transfer device operating in the same way as the HP. Heat supplied to evaporator makes a

*Address correspondence to this author at the Saga University, Graduate school of Science and Engineering, Saga, Japan;
Tel: +81-952-28-8623
E-mail: miyara@me.saga-u.ac.jp

E-ISSN: 2409-5826/19 

liquid turn into vapor, then flow to the condenser where vapor releases heat to the heat sink and becomes liquid again. However, in the LHP vapor and liquid phases flow in separated tubes where are no capillary structure or wick placed on, but porous wick is only installed in evaporator, so the LHP can avoid entrainment limit and operate with the lower pressure loss to circulate the working fluid comparing to the conventional HP. Consequently, the LHP has the higher heat transfer capacity, smaller thermal resistance and more flexible characteristics than normal HP [5]. Besides, working fluid is circulated inside the LHP by the capillary or gravity effect, no mechanical component functioning is required like the other active two-phase cooling methods. It means that both of electricity consumption and operating cost can be reduced while the lifespan and reliable performance can be higher. Moreover, in the fields of DCs thermal management, it is feasible to arrange the position of evaporator lower than condenser to utilize the gravity in circulating the fluid, or the cooling capacity can be gained dramatically than when LHP operates horizontally or anti-gravity condition.

Because of passive operating characteristics, LHP's performance is influenced by various factors that are properties of working fluid, filling ratio, wick's characteristics, cooling and ambient condition, geometric designs of the component [6]. Despite that, the selection of working fluid can be one of the most important parameters because the appropriate working fluid can improve the heat transfer processes in the evaporator and condenser of the LHP or minimize the pressure loss caused by the circulation, so increase the cooling capability. There are many criterions for selecting a working fluid such as the compatibility with LHP's material, good thermal stability, wettability characteristic, suitable operating pressure, high Merit number ($\sigma_l \rho_l h_{fg}/\mu_l$), and etc [7]. In addition, the fluid working in the LHP should also have the high value of derivative $dP/dT$ for the ensuring the LHP start up and operation [5]. Therefore, it is difficult to find out the working fluid that can satisfied all above requirements, but it is important to understand the way that the working fluids effect on performance of not only the LHPs but also each components belonging to the LHP; so, it is possible to find out the appropriate design that can balance the advantage and disadvantage points of each working fluid used in the LHP.

In this study, the experiment with the LHP operating under gravity assisted condition and the precision measuring instruments was established to investigate the thermal performance of the LHP, the heat transfer characteristics at the evaporator and condenser when water and ethanol were working fluid respectively. This LHP aims to cool the electronics devices like processors, so the evaporator has the flat-rectangular shape as described in Figure **1** to contact well with the electronics surface. The evaporator consists of three main parts that are stainless-steel (SS) lid (8), copper base (4) and SS body (5). Despite operating with gravitational favour, the LHP's evaporator also includes a commercial porous SS wick (3) functioning as the hydraulic barrier which assures that the fluid circulates stable in one direction. Besides, above the wick is the compensation chamber (7) which ensures the liquid supplied to evaporator and tolerates the liquid when LHP operates at different heating power. There is the crossing grooves system, or the array of fins, machined on the inner surface of the evaporator base (4). This design can avoid machining the grooves on wick surface but assure not only the space for evaporation but also adequate paths for vapor to flow out evaporator easily. The experimental results indicate that in general, the water LHP has the better cooling performance than ethanol LHP except for the low heating power region. Furthermore, the discussion about the difference in boiling and condensation heat transfer of water and ethanol LHP are introduced in this paper.

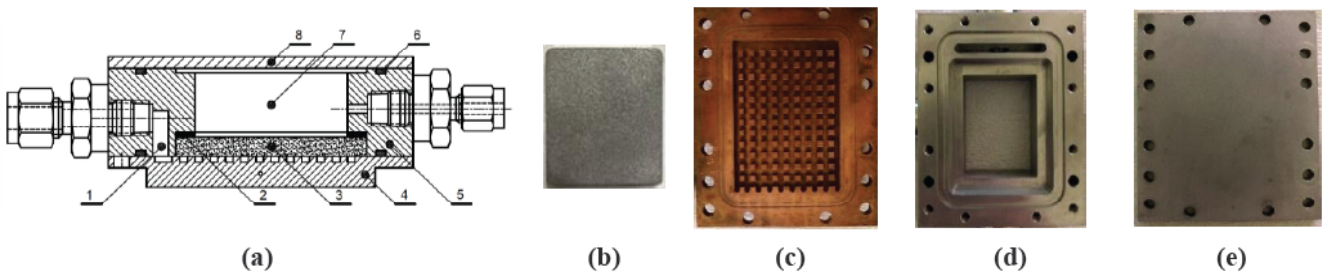


**Figure 1: (a)** Evaporator structure: vapor collector (1), silicone gasket (2), SS wick (3), copper base (4), SS body (5), O-ring (6), compensation chamber (7), SS lid (8); **(b)** Stainless steel sintered wick; **(c)** copper base of evaporator; **(d)** SS body; **(e)** SS lid.

## 2. EXPERIMENTAL SETUP & DATA REDUCTION

### 2.1. Experimental Setup and Charging System

#### *2.1.1. Schematic Diagram of Experiment*

**Table 1: The Main Parameters of LHP**

| | |
|---|---|
| **Heating block** | Copper |
| Mass, kg | 4.36 |
| **Evaporator base** | Copper |
| Length x Width x Height, mm | 80 x 66 x 8 |
| Active area, $mm^2$ | 60 x 45 |
| **Evaporator body** | Stainless steel |
| Length x Width x Height, mm | 80 x 68 x 23 |
| **Fin geometry** | |
| Cross area, $mm^2$ | 2 x 2 |
| Height, mm | 1.5 |
| Fin pitch, mm | 4 |
| **Wick structure [8]** | Stainless steel |
| Opening, μm | 63 |
| Void ratio, % | 42 |
| Bulk volume, $mm^3$ | 50 x 41 x 5 |
| **Compensation chamber** | |
| Length x Width x Height, mm | 40 x 31 x 18 |
| **Vapor line** | Copper |
| OD/ID, mm | 6.35/4.35 |
| Length, mm | 725 |
| **Condenser line** | Copper |
| OD/ID, mm | 6.35/4.35 |
| Length, mm | 600 |
| **Liquid line** | Copper |
| OD/ID, mm | 6.35/4.35 |
| Length, mm | 110 |
| OD/ID, mm | 3.2/1.7 |
| Length, mm | 1200 |
| **Working fluid amount (ml)** | |
| Ethanol | 36 |
| Water | 34.5 |

Table **1** lists the main design parameters of the LHP and the experimental schematic diagram is shown in Figure **2.** Heat generated from electronics was simulated by four cartridge heaters inserted inside the copper heating block while its magnitude was adjusted and monitored by the YAMABISHI MVS-520 volt-slider and YOKOGAWA WT230 digital power meter respectively. On the other hand, heat released from

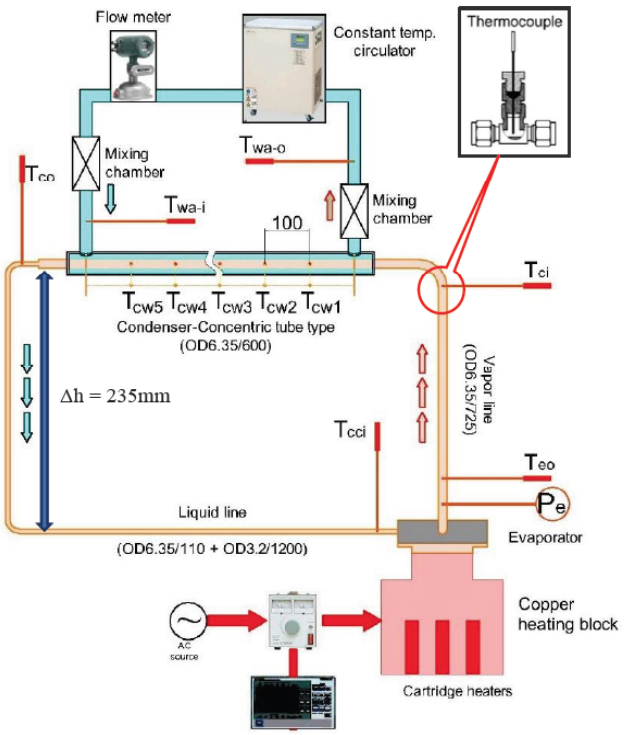


**Figure 2:** Schematic diagram of experiment.

condenser was taken by the water of which temperatures at the condenser inlet and mass flow rate were controlled at 25°C and 35 kg/h by the ADVANTEC LV-400 constant temperature circulator device. For understanding the state of working fluid inside LHP, four sheath K-type thermocouples including $T_{eo}$, $T_{ci}$, $T_{co}$, $T_{cci}$ were inserted directly to the LHP at the outlet of evaporator, inlet of condenser, outlet of condenser and inlet of compensation chamber respectively. Besides, there were five T-type thermocouples from $T_{cw1}$ to $T_{cw5}$ fixed on the outer wall of condenser to find out temperature distribution. One pressure transducer $P_e$ was installed at the outlet of evaporator to measure the vapor pressure. Although the digital power meter could indicate the heating power generated by heaters, the accurate value was estimated from the temperature gradient measured by three 0.5mm sheath K-type thermocouples inserted to the copper heating block (Figure **3**). Further, to estimate the thermal contact resistance as well as the temperature at the base's fin, an 1mm sheath K-type thermocouple $T_4$ was installed at the evaporator base. Finally, heat released from condenser was determined from mass flow rate and the temperature different of cooling water that was measured by the MASSMAX MMM7150K mass flow meter and two K-type thermocouples $T_{wa-i}$ and $T_{wa-o}$. All measured data were collected and recorded by the KEITHLEY 2701 data acquisition system.

**Table 2: Uncertainty Values**

| | Uncertainty |
|---|---|
| $T_1$, $T_2$, $T_3$ | ±0.06°C |
| $T_4$ | ±0.07°C |
| $T_{eo}$, | ±0.06°C |
| $T_{ci}$, | ±0.06°C |
| $T_{co}$, $T_{cci}$ | ±0.1°C |
| $T_{wa\text{-}i}$, | ±0.1°C |
| $T_{wa\text{-}o}$ | ±0.06°C |
| $T_a$ | ±0.16°C |
| $T_{cw}$ | ±0.1°C |
| Pressure transducer | ±1.5 kPa |
| Mass flow meter | 0.18% of reading |

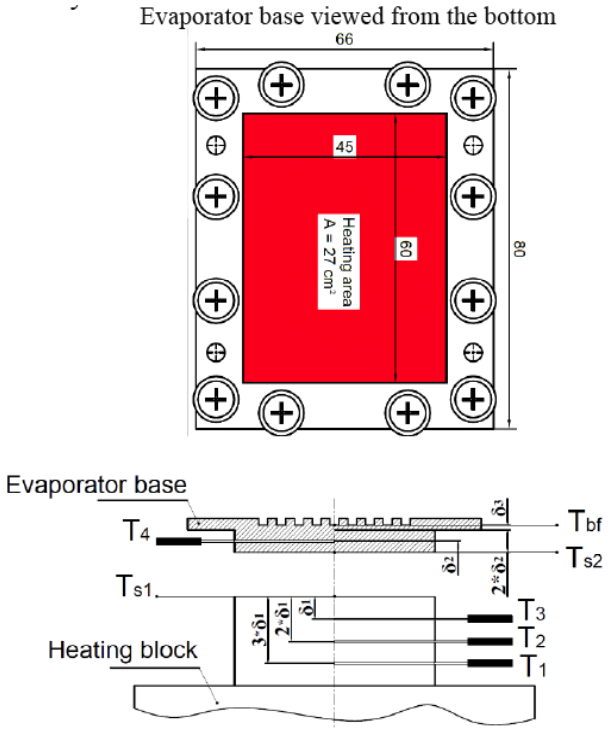


**Figure 3:** Temperature gradient measurement.

The uncertainty values of measuring devices are listed in Table **2.** The uncertainties of the thermo-couples were obtained from the calibration process in which Pt100 thermometer (Chino Co. Model – R900-F25AT) was the used as the standard source.

### *2.1.2. Charging System and Charging Procedure*

Figure **4** explains the vacuum and charging system of the LHP. The first step is closing the valve $V_1$, then vacuuming the whole volume of the charging system and LHP by the ULVAC GLD-051 pump. The vacuum duration was almost longer than 1 day. The next step is to disconnect the LHP and the charging tank by closing the valve $V_2$, $V_5$, $V_6$, opening the valve $V_1$ to make the working fluid from the syringe flow down into the charging tank. The working fluid can enter the charging tank due to the difference between atmosphere pressure above the syringe and the vacuum pressure inside the tank. The valve $V_1$ is closed after finishing this step. To eliminate the non-condensable gas dissolved in the working fluid, the charging tank is heated to boil the liquid inside and vacuum again. Finally, the valve $V_6$ is opened for working fluid flow into the LHP. The amount of working fluid charged to the LHP is adjusted by the charging regulator valve and observing the changing of liquid level on the glass level indicator. Distilled water (Kanto Chemical Co.) and ethanol (99.5% - Kishida Chemical Co.) were working fluids in this study.

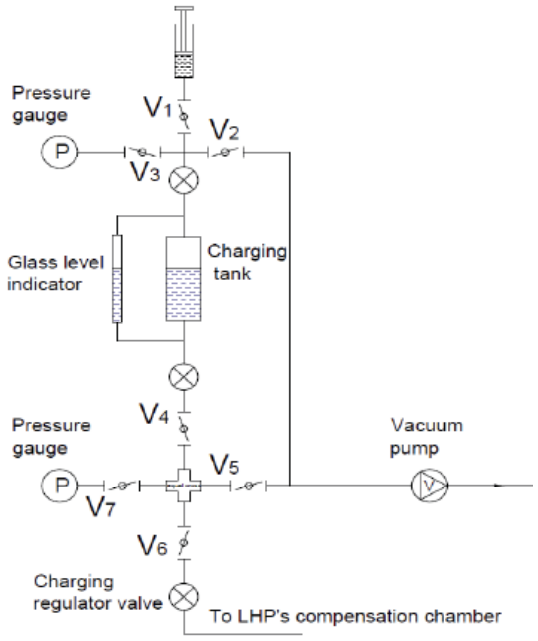


**Figure 4:** Charging and vacuum system for LHP experiment.

### 2.2. Data Reduction

From Figure **3**, the values of heat flux q and heat flow rate Q flowing from the heating block to the evaporator can be estimated as follows

$$q = \frac{1}{3}\left(k\frac{\Delta T_{12}}{\delta_1} + k\frac{\Delta T_{23}}{\delta_1} + k\frac{\Delta T_{13}}{2\delta_1}\right) \quad (1)$$

$$Q = q * A \quad (2)$$

With:

- $\delta_1$ = 5 mm, distance between the thermocouples $T_1$, $T_2$, $T_3$
- A = 27 cm$^2$, area of the top surface of the heating block and active area of the evaporator. This area was selected basing on the common size of the processors functioning in the DC (Intel® core™ i9-9900k processor: 37.5 mm x 37.5 mm; Intel Xeon E7 8891 v3: 52 mm x 45 mm)

Besides, temperature at the top surface of heating block $T_{s1}$

$$T_{s1} = \frac{1}{3}\left[\left(T_1 - \frac{3(q\delta_1)}{k}\right) + \left(T_2 - \frac{2(q\delta_1)}{k}\right) + \left(T_3 - \frac{(q\delta_1)}{k}\right)\right] \quad (3)$$

From thermocouple $T_4$, temperature at the bottom of evaporator $T_{s2}$ can be determined

$$T_{s2} = T_4 + \frac{q\delta_2}{k} \quad (4)$$

With:

- $\delta_2$ = 2.5 mm, distance between the evaporator bottom surface and the thermocouples $T_4$

The values of total thermal resistance $R_t$, evaporator thermal resistance $R_e$, condenser thermal resistance $R_c$, and thermal contact resistance $R_{ct}$ were estimated by the following equations

$$R_t = \frac{T_{s1} - T_{wa-i}}{Q} \quad (5)$$

$$R_e = \frac{T_{s2} - T_{eo}}{Q} \quad (6)$$

$$R_c = \frac{T_{ci} - T_{wa-i}}{Q} \quad (7)$$

$$R_{ct} = \frac{T_{s1} - T_{s2}}{Q} \quad (8)$$

In the experiment, because vapor flows in the vapor pipe at high velocity and the vapor pipe was insulated well, the process vapor flow from outlet of evaporator to inlet of condenser can be recognized as adiabatic process, and temperature difference between $T_{eo}$ and $T_{ci}$ is not noticeable; therefore

$$R_t = R_e + R_c + R_{ct} \quad (9)$$

In this study, the values of evaporator heat transfer coefficient (HTC) could be determined from two correlations, the first one $h_{e\text{-}T}$ was estimated from thermocouple $T_{eo}$ locating at the outlet of evaporator and the other $h_{e\text{-}P}$ was calculated from the saturation temperature $T_{sat\text{-}P}$ accessed from the vapor pressure $P_e$ by REFPROP Ver. 9.1.

$$h_{e-T} = \frac{q}{T_{bf} - T_{eo}} \quad (10)$$

$$h_{e-P} = \frac{q}{T_{bf} - T_{sat-P}} \quad (11)$$

As shown in Figure **3**, $T_{bf}$ is the temperature at the base of the fins that could be estimated by Eq (12)

$$T_{bf} = T_4 - q\left(\frac{\delta_2}{k} + \frac{A\delta_3}{kA'}\right) \quad (12)$$

With: A, A', $\delta_2$, $\delta_3$ are the dimensions displayed in Figure **3**

- A = 27 cm$^2$, active area of the evaporator
- A' = 52.8 cm$^2$, the area determined from the outer dimension of the evaporator
- $\delta_2$ = 2.5 mm; $\delta_3$ = 1 mm

## 3. RESULTS AND DISCUSSION

### 3.1. Cooling Capacity and Performance of Water LHP and Ethanol LHP at Different Heating Power

Figure **5 & 6** demonstrates the changes of the temperatures such as $T_{s1}$ at the top surface of the heating block, temperatures at different positions in the LHP including $T_{eo}$, $T_{ci}$, $T_{co}$ and $T_{cci}$ on the heating power when LHP was charged with water and ethanol. As the whole, water LHP performed better than ethanol LHP except for the range of heat power lower than 90 W. The water LHP could maintain the value of $T_{s1}$ to not higher than 110$^o$C when operating in the range of heating power from 33 to 535 W. However, in the experiment of ethanol LHP, this parameter reached 133$^o$C when heating power was adjusted at the value of 395 W. If $T_{s1}$ is regarded as the operating temperature of the electronics, normally it is suggested that this temperature should not be higher than 85$^o$C to guarantee the reliable and effective operation of electronic devices [9]. The ethanol LHP could satisfy this limitation when functioning at the heating power of 220 W, but the water LHP could do the same thing when cooling the electronics generating the heat at the rate of 350 W.

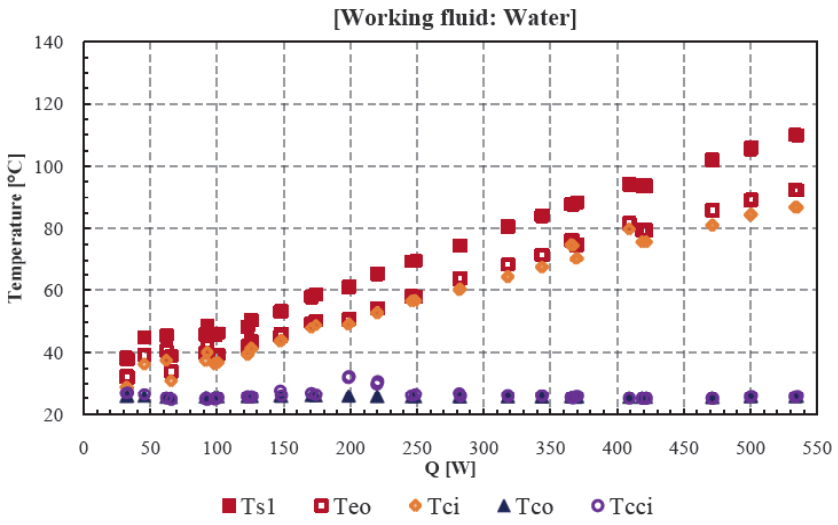


**Figure 5:** Changing of $T_{s1}$ and LHP's temperatures on heating power when LHP was charged with water.

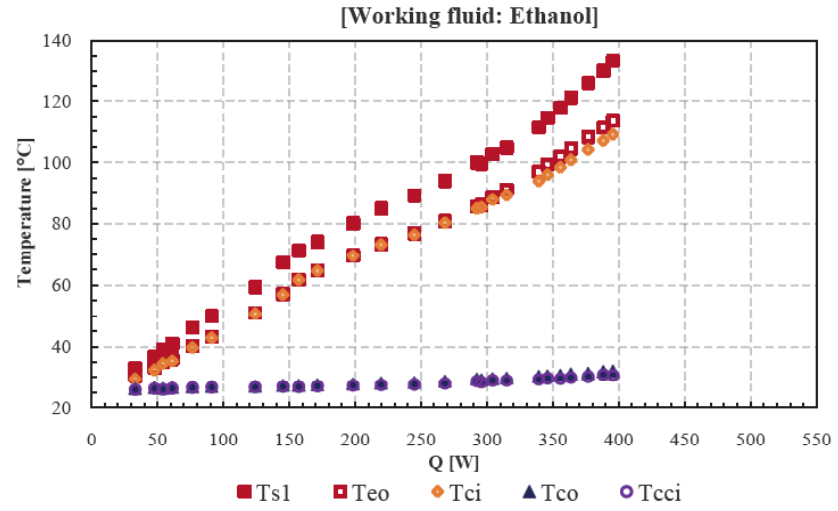


**Figure 6:** Changing of $T_{s1}$ and LHP's temperatures on heating power when LHP was charged with ethanol.

Through the temperature distribution of working fluid at different positions in the LHP, both water LHP and ethanol LHP achieved the stable operation on the whole range of heating power. However, the water LHP behaved some fluctuations in the range of heating power from 150 to 250 W where the values of $T_{cci}$ were slightly higher than $T_{co}$. This result indicates that there was the intermittent appearance of vapor-liquid interface near the position of thermocouple $T_{cci}$ on the liquid line. This phenomenon was not observed in the experiment of ethanol LHP. It means that the supplying liquid for the compensation chamber is more stable than water LHP. Despite that, there was no significant difference between $T_{co}$ and $T_{wa-i}$ in the experiment of water LHP, but this temperature difference became larger with heating power in the case of ethanol LHP. This result shows that the cooling performance of the condenser operating with ethanol was less effective than one with water. It is one of the reasons that make the ethanol LHP could not working as powerfully as the water LHP could.

### 3.2. Change of Thermal Resistances with Heating Power

#### *3.2.1. Change of Total Thermal Resistances with Heating Power*

Figure **7** demonstrates how total thermal resistance $R_t$ of the water LHP and ethanol LHP varied with the heating power. It agrees with previous discussion that water LHP operates better than ethanol LHP when heat was supplied to the evaporator more than 90 W. With the water LHP, the values of $R_t$ changed within the tendency that became smaller with the increase of heating power, especially it reduced significantly from

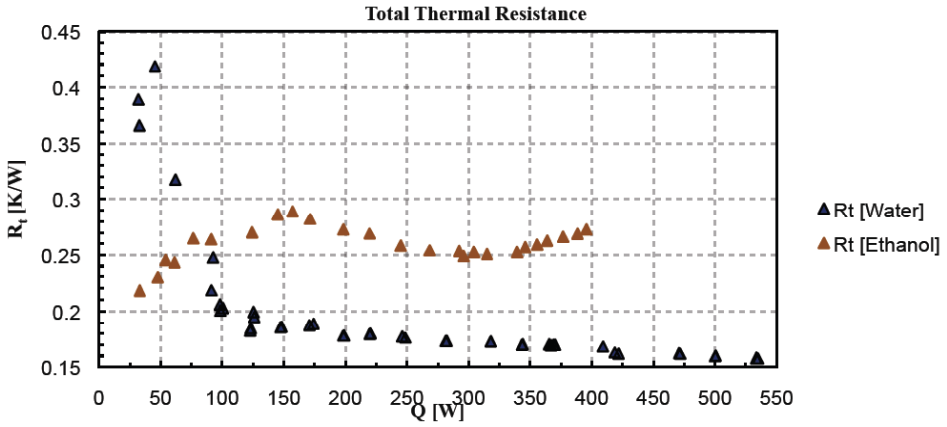


**Figure 7:** Changing of total thermal resistance of water and ethanol LHP on heating power.

0.418 to 0.2 K/W when heat supplied to the evaporator increased from 30 to 100 W. At the heating power of 535 W, this thermal resistance had the value of 0.159 K/W. On the other hand, the change of total thermal resistance $R_t$ with the heating power obtained from the ethanol LHP was not like what behaved by the water LHP. Only in the range of heating power from 150 to 300 W, the values of $R_t$ reduced with the increasing of heating power, while it almost raised up under the rest operating conditions. The ethanol LHP had the minimum value of $R_t$ at 0.218 K/W when functioning at the heating power of 33W. The following sections explain more detail about the difference in performance at each components of water LHP and ethanol LHP.

### *3.2.2. Change of the Evaporator Thermal Resistances with Heating Power*

The variation of evaporator thermal resistance $R_e$ with heating power values in the experiment of water LHP and ethanol LHP is displayed in Figure **8**. As the whole, the evaporator behaved almost same characteristics when working with water and ethanol respectively. In the range of heating power from 90 to 300 W, there was no notable difference in both of values and changing tendency of thermal resistance values between the evaporator when functioning with water and ethanol. In this region, the higher heating power was generated from the heaters, the smaller values of evaporator thermal resistance became. However, there were still some distinct behaviors happening. The evaporator operating with ethanol was more effective than one with water when heating power was not higher than 90 W. Further, in the range that heating power was higher than 300 W, when raising up the heat, the ethanol evaporator increased its thermal resistance while thermal resistance of water evaporator continued decreasing little. Besides, observing Figure **7** and **8**, it can be concluded that in the case of ethanol LHP, the performance of the evaporator affected on total performance of the LHP weakly, particularly in the range of heat power from 33 to 150 W. On the other hand, with the water LHP, the high thermal resistance of the evaporator contributed significantly to the total

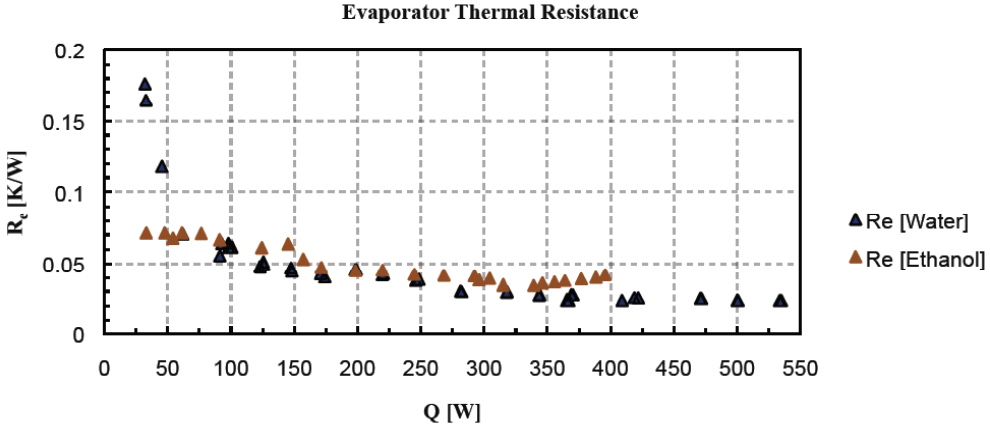


**Figure 8:** Changing of evaporator thermal resistance of water and ethanol LHP on heating power.

thermal resistance of LHP when heating power was less than 90 W.

### *3.2.2. Change of the Condenser Thermal Resistances with Heating Power*

The effect of heating power on the condenser in ethanol LHP and water LHP is presented in Figure **9**. Comparing to Figure **7**, it can be concluded that the thermal performance of the LHPs was dominated strongly by the heat transfer process at the condenser, especially in the case of the LHP charged with ethanol. The high thermal resistance existing at the condenser of the ethanol LHP can be recognized as the main reason causing the cooling capacity of this LHP is lower than water LHP. Moreover, the tendencies that the condenser thermal resistance varied with the heating power were clearly different in the cases that water and ethanol were charged to the LHP. With the water LHP, the values of $R_c$ reduced strongly within the low heating power region and was almost constant in the high heating power range, but the thermal resistance of the condenser in the ethanol LHP raised up when heating power was increased. This result can be explained from the difference in the thermal properties of water and ethanol. Basing upon the Chato correlation [10], because water has higher latent heat and liquid thermal conductivity, at the same rate of heat released from condenser the thickness of ethanol liquid condensing must be more than in the case of water and this layer becomes the resistance preventing the heat transfer process from the vapor to cooling water. Moreover, the low vapor density of water that makes vapor flow at higher velocity is also another reason that explains why the condenser working with water have the lower thermal resistance.

In this experiment, 5 T-types thermocouples were fixed on the outer wall of condenser to detect the temperature distribution along the length of the condenser, and the measured data are shown in Figure **10**. The condenser working with water had the shorter two-phase flow region or the heat transfer area

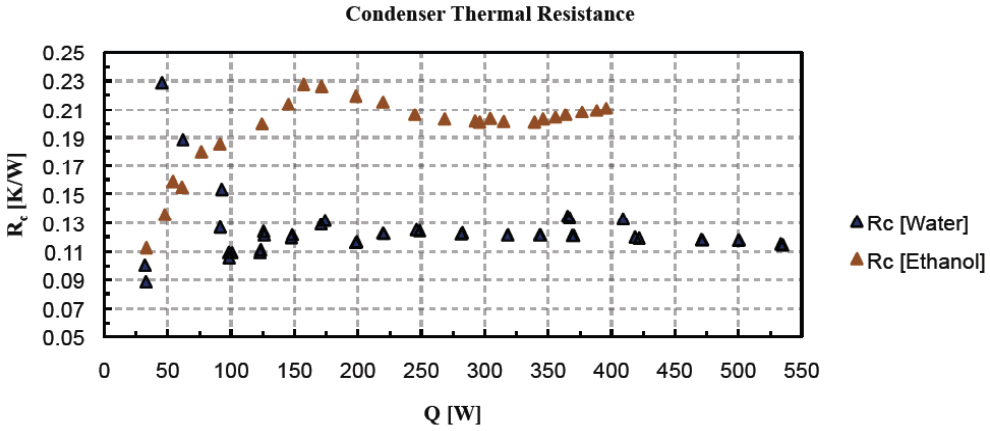


**Figure 9:** Changing of condenser thermal resistance of water and ethanol LHP on heating power.

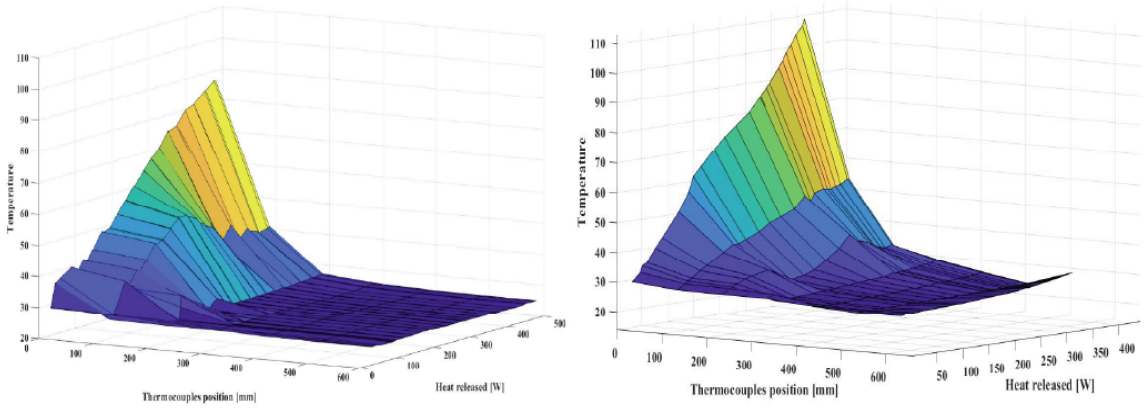


**Figure 10:** Temperature distribution on the outer wall of condenser (a) water LHP (b) ethanol LHP.

Thermocouples' positions:
0 mm: $T_{ci}$, 100 mm: $T_{cw1}$, 200 mm: $T_{cw2}$, 300 mm: $T_{cw3}$, 400 mm: $T_{cw4}$, 500mm: $T_{cw5}$, 600 mm: $T_{co}$

for condensation being smaller than one working with ethanol. However, at the low heating power condition, condensation of water also took half of the condenser's length or the pressure loss became higher that could increase the pressure and saturation temperature of vapor before entering the condenser. Consequently, the condensation thermal resistance would be higher under this heating power condition.

### *3.2.2. Change of the Thermal Contact Resistances with Heating Power*

Though both the evaporator's bottom and the top surface of heating block are the flat surfaces, and a thin layer of thermal conductivity grease was used to minimize the thermal resistance caused by contact condition, it is impossible to ignore this resistance. The results in Figure **11** shows that values of thermal contact resistance $R_{ct}$ at various heating power in both experiments of water LHP and ethanol LHP were not notably different and mostly changed in the range from 0.006 K/W to 0.0092 K/W. Although the experiment of ethanol LHP and water LHP were conducted separately, the $R_{ct}$ in two cases had almost same value or this thermal resistance had the same effect on the cooling capacity of ethanol and water LHP

## 3.3. Evaporator HTC and the Boiling Characteristics of Evaporator Operating with Water and Ethanol

In this study, the evaporator HTC was estimated from the vapor temperature $T_{eo}$ at the outlet of

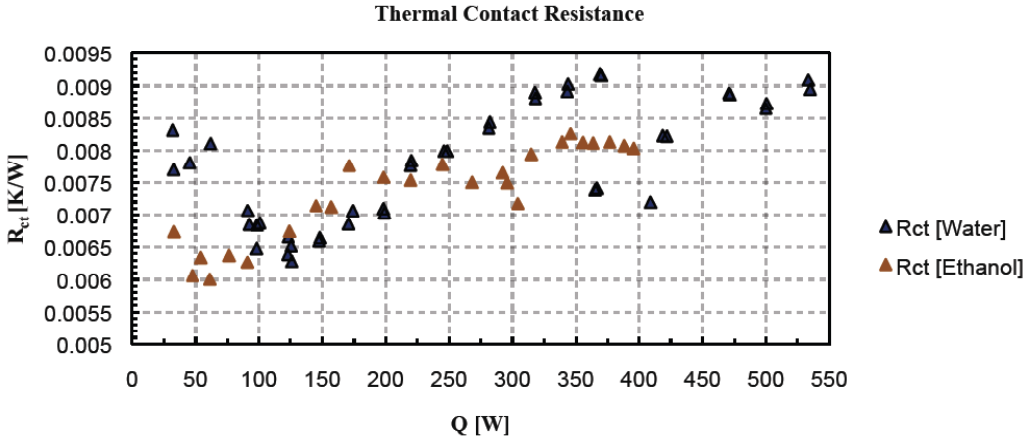


**Figure 11:** Thermal contact resistance.

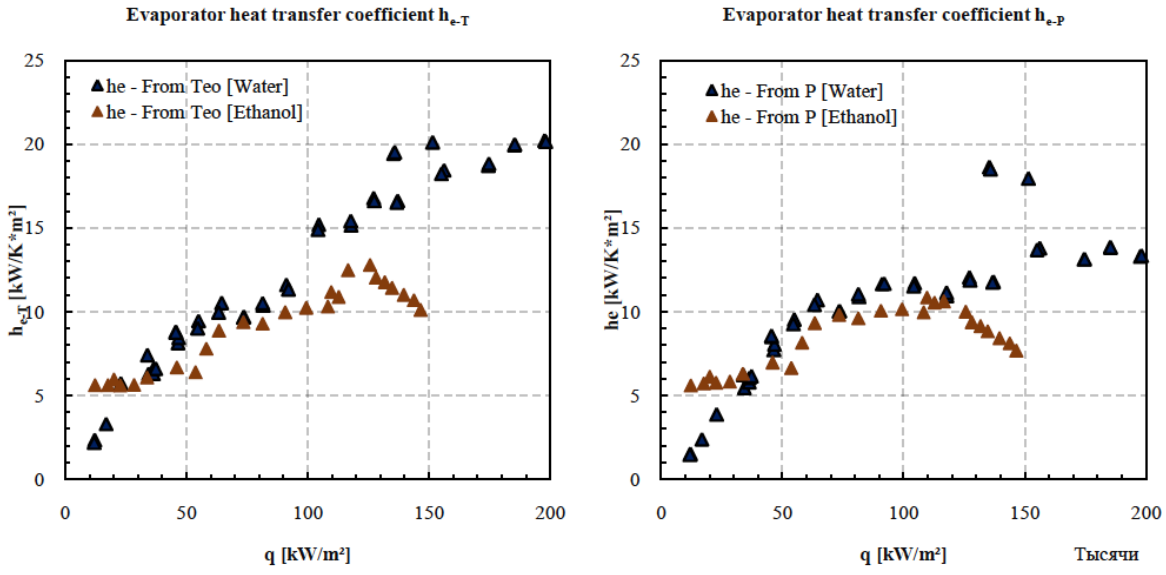


**Figure 12:** Evaporator HTC in the in the experiments of water LHP and ethanol LHP.

a) Estimated from temperature at the outlet of evaporator $T_{eo}$
b) Estimated from saturated temperature $T_{sat-P}$

evaporator and the saturation temperature $T_{sat-P}$ obtained from the vapor pressure measured at the outlet of evaporator. In the range of heat flux lower than 100 kW/m$^2$, there was no notable difference between the results determined by the two Eq (10) & (11) in both experiments of water LHP and ethanol LHP. It indicates that the vapor flowing out the evaporator almost existed at the saturated state without superheated process. When heat flux was increased to be higher than 100 kW/m$^2$, evaporator HTC obtained from $T_{eo}$ was higher than values calculated from saturation temperature $T_{sat-P}$. The difference in the results shows that the vapor might be superheated before leaving the evaporator. This superheating process could happened when vapor flow in the crossing grooves, and the heat of this process came from the surrounding area of the fins and the grooves' surface. In addition, with the method of thermocouple installation shown in Figure **2**, and the distance between thermocouple $T_{eo}$ and the evaporator is 125 mm, the heat conduction from evaporator to the thermocouple can be negligible. From this explanation, it can be withdrawn that with this design of evaporator when the heat flux is higher than 100 kW/m$^2$, the working fluid almost boiled on the fin's tip surface or the contact area between the wick and the fin This result also confirms the assumption of boiling characteristics in this evaporator that was introduced in previous paper [11].

Comparing the evaporator HTC of the in the experiment of water LHP and ethanol LHP, the evaporator operating with ethanol had the higher evaporator HTC when the heat flux was smaller than 30 kW/m$^2$. The high surface tension of water could make the formation and growing of the bubble more difficult under small heat flux condition; consequently, it requested the excess temperature to be higher for the boiling to happen. In the range of 30 to 100 kW/m$^2$ heat flux, the evaporator HTC of water LHP was higher than values of ethanol LHP a little. The noticeable difference occurred when the value of heat flux was higher than 100 kW/m$^2$. Because the HTC calculated from Eq (10) does not include the superheated process, the performance of the evaporator should be discussed based upon the results shown in Figure **12 (b)**. When functioning under this condition, the evaporator HTC in the experiment of water LHP increased little with the increment of heat flux, but this parameter reduced in the case of ethanol LHP. The dissimilar performance can be explained by the assumption described in Figure **13**.

As mentioned in the above discussion, when heat flux was larger than 100 kW/m$^2$, the boiling almost happened at the surfaces where the wick and the fin contact together. Because of this characteristic, the evaporator HTC will be influenced by some

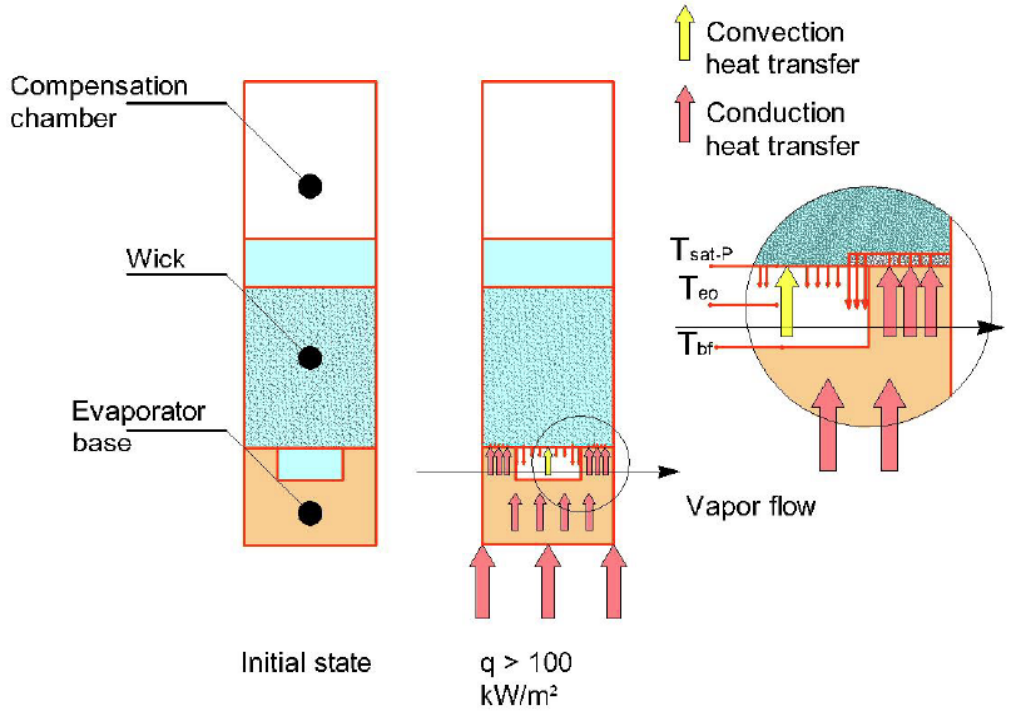


**Figure 13:** Assumption about boiling heat transfer mechanism under condition that heat flux is higher than 100 kW/m$^2$.

disadvantage sides such as the heat flux on the fin's tip became higher, and a thin layer of vapor that may form on the tip surface of the fin makes the liquid more difficult in receiving heat for evaporation. Particularly, in the case of ethanol because of the small surface tension, it could not create the menisci having sufficient area for the evaporation as the liquid having high surface tension like water can do. Consequently, the ethanol vapor layer could be thicker and excess temperature becomes higher. Furthermore, the convection heat transfer is also an aspect that should be focused. Although almost heat had to flow through the fin to the liquid in the wick by conduction, there was some heat transferred to the wick by convection and radiation as displayed in Figure **13**. This mechanism of heat transfer could improve the boiling characteristic by promoting the boiling happening on the non-contact surface of the wick. It means that the wick surface can be utilized effectively for the boiling, so the "boiling load" on the contact surfaces could be reduced. If the effect of radiation was regarded to be similar, the difference in convection heat transfer when water and ethanol were working fluid also contributed to making the evaporator behave differently. Because ethanol has the product of ($h_{fg}\rho_v$) higher than water, at the same heat flux the vapor velocity flow through the groove will be slower than the water vapor. As the results, the promotion of boiling by the convection in the case of ethanol LHP was weaker than water LHP. The above assumption can be used to explain why under the condition that heat flux was more than 100 kW/m$^2$, the evaporator HTC in the experiment of water LHP increased slightly with the increment of heat flux while this parameter reduced in the ethanol LHP's experiment.

## CONCLUSION

In this study, an LHP with flat-rectangular evaporator was fabricated and investigated its performances when working with two different fluids including water and ethanol. All of the experiments were conducted under the same condenser cooling condition. The experimental results demonstrate that as a whole, the water LHP has the better cooling performance than ethanol LHP except for the range of heating power lower than 90 W. The water LHP could maintain the temperature at the top surface of the heating block smaller than 85$^o$C when operating under heating power of 350 W; on the other hand, the ethanol LHP could satisfy this condition when the heating power was around 220 W only. Among various components of thermal resistance, the condenser thermal resistance was the component that dominates most on the LHP's performance, especially in the case of the ethanol LHP. For the water LHP, at the low heating power operating condition, the evaporator thermal resistance also contributed significantly to the total thermal resistance of the LHP because the high surface tension characteristic that could make the formation and growing process of the bubble difficult. In addition, the results of the evaporator HTC obtained from the experiments of water and ethanol LHP in this study also confirmed for the assumption of boiling heat transfer characteristics that presented in the previous study. Moreover, the effect of convection heat transfer on the performance of the evaporator when heat flux was more than 100 kW/m$^2$ was also discussed in this paper.

## NOMENCLATURE

### Abbreviations

DC : data center

LHP : loop heat pipe

SS : stainless steel

HTC : heat transfer coefficient

$A$ : area of the top surafce of the heating block, m$^2$

$c_p$ : specific heat of cooling water, J/(kgK)

$h_{e-T}$ : evaporator HTC, estimated from $T_{eo}$, kW/(m$^2$K)

$h_{e-P}$ : evaporator HTC, estimated from $P_{eo}$, kW/(m$^2$K)

$h_{fg}$ : latent heat, kJ/kg

ID/OD : pipe inner, outer diameter, mm

$k$ : copper thermal conductivity, W/(m·K)

$m_{wa}$ : cooling water mass flow rate, kg/s

$q$ : heat flux, kW/m$^2$

$Q$ : heating power, W

$Q_c$ : heat released from condenser, W

$R_{t,}$ : total thermal resistance, K/W

$R_{e,}$ : evaporator thermal resistance, K/W

$R_{c,}$ : condenser thermal resistance, K/W

$R_{ct}$ : thermal contact resistance, K/W

$T_1$ to $T_3$ : heater temperature, $^oC$

$T_4$ : evaporator base temperature, $^oC$

$T_a$ : room temperature, $^oC$

$T_{bf}$ : temperature at the base of fin, $^oC$

$T_{ci}$ : temperature at condenser inlet, $^oC$

$T_{co}$ : temperature at condenser outlet, $^oC$

$T_{cci}$ : temperature at compensation chamber inlet, $^oC$

$T_{cw1}$ to $T_{cw5}$ : condenser outer wall temperature, $^oC$

$T_{eo}$ : temperature at evaporator outlet, $^oC$

$T_{s1}$ : temperature at heater surface, $^oC$

$T_{s2}$ : temperature at evaporator bottom surface, $^oC$

$T_{wa-i}$ : temperature of cooling water at inlet position, $^oC$

$T_{wa-o}$ : temperature of cooling water at outlet position, $^oC$

$\delta_1$ : distance between the thermocouples inside heating block, m

$\delta_2$ : distance between the thermocouple $T_4$ and the bottom surface of evaporator, m

$\rho_l$ : liquid density, $kg/m^3$

$\rho_v$ : vapor density, $kg/m^3$

$\sigma$ : surface tension, N/m

$\mu$ : viscosity, Pa.s

## REFERENCES


[1] Sohel Murshed SM and Nieto de Castro CA. A critical review of traditional and emerging techniques and fluids for electronics cooling. Renew. Sustain. Energy Rev 2017; 78: 821-33. https://doi.org/10.1016/j.rser.2017.04.112

[2] Nadjahi C, Louahlia H and Lemasson S. Sustainable Computing : Informatics and Systems. Sustain. Comput. Informatics Syst 2018; 19: 14-28. https://doi.org/10.1016/j.suscom.2018.05.002

[3] Habibi A and Halgamuge SK. A Review on e ffi cient thermal management of air- and liquid-cooled data centers : From chip to the cooling system. Appl Energy 2017; 205: 1165-88. https://doi.org/10.1016/j.apenergy.2017.08.037

[4] Zhang H, Shao S, Xu H, Zou H and Tian C. Free cooling of data centers : A review 2014; 35: 171-82.

[5] Maydanik YF. Loop heat pipes. Applied Thermal Engineering 2005; 25: 635-657. https://doi.org/10.1016/j.applthermaleng.2004.07.010

[6] Launay S, Sartre V and Bonjour J. Parametric analysis of loop heat pipe operation : a literature review. International Journal of Thermal Sciences 2007; 46: 621-36. https://doi.org/10.1016/j.ijthermalsci.2006.11.007

[7] David Reay RM, Peter Kew. Heat Pipe Theory, Design, and Applications, 6th ed. Butterworth-Heinemann 2014.

[8] SMC Cooperation, Sintered metal element (EB/ES Series) pp. 103-118 https://www.smcworld.com/products/-en/s.do?ca_id=537 (accessed Nov. 27th,2017)

[9] Ebrahimi K, Jones GF and Fleischer AS. A review of data center cooling technology, operating conditions and the corresponding low-grade waste heat recovery opportunities. Renew. Sustain. Energy Rev 2014; 31: 622-38. https://doi.org/10.1016/j.rser.2013.12.007

[10] Incropera DP, Frank P, DeWitt. Fundementals of heat and mass transfer. 6th ed. John Wiley & Sons 2007.

[11] Phuoc Hien Huynh, Kyaw Zin Htoo, Tuhin AR, Keishi Kariya. Akio Miyara "Experimental study on thermal performance and boiling heat transfer of loop heat pipe operating under gravity assisted condition," in 2017 JSRAE Annual Conference, p. E221.


Received on 12-10-2018 Accepted on 6-12-2018 Published on 10-6-2019

DOI: http://dx.doi.org/10.15377/2409-5826.2019.06.3